SHANGHAI JIAO TONG UNIVERSITY

ATLAS EXPERIMENT

Tsung-Dao Lee Institute

Search for triple Higgs boson production in the 6b final state at 13TeV with the ATLAS detector

Jing Chen

2024 .12.22

Higgs Potential 2024

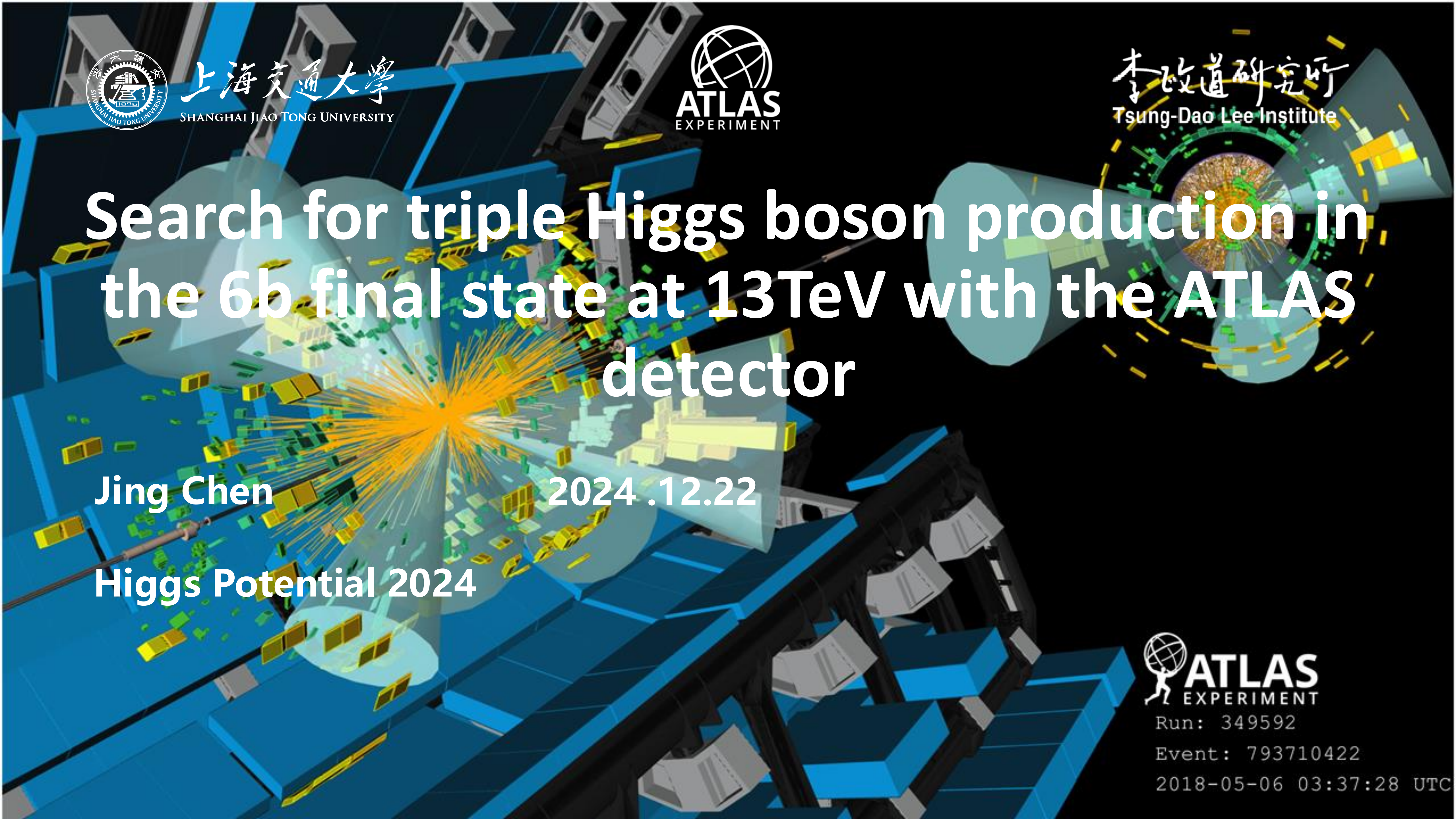

$HHH \rightarrow 6b$

- HIGGS POTENTIAL

$$V(H) = \frac{1}{2}m_H^2H^2 + \lambda_3 v H^3 + \lambda_4 H^4 + O(H^5)$$

  - SM tri-Higgs production is sensitive to tri-linear and quartic Higgs self-couplings (λ_3 & λ_4).
  - Constrain modifications to SM coupling values (κ_3 & κ_4- no experimental bounds before).
  - Quartic couplings can only be accessed directly this way.

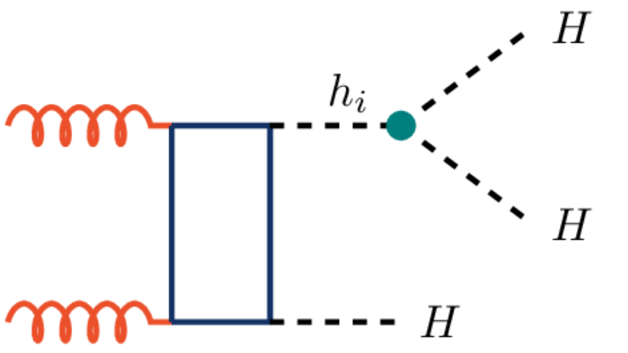

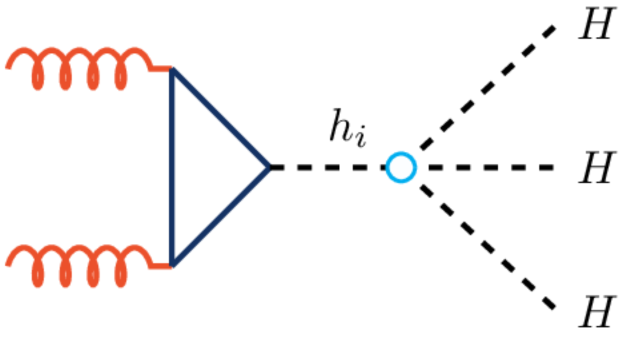

- Small SM tri-Higgs ggF production cross-section at $\sqrt{s}$=13TeV : $\sim$ 0.079fb at NNLO.

- Some BSM theories predict nontrivial tri-Higgs production.

- Rare process → 6b final state (large branching ratio: $H \rightarrow b\bar{b}$ ~58%).

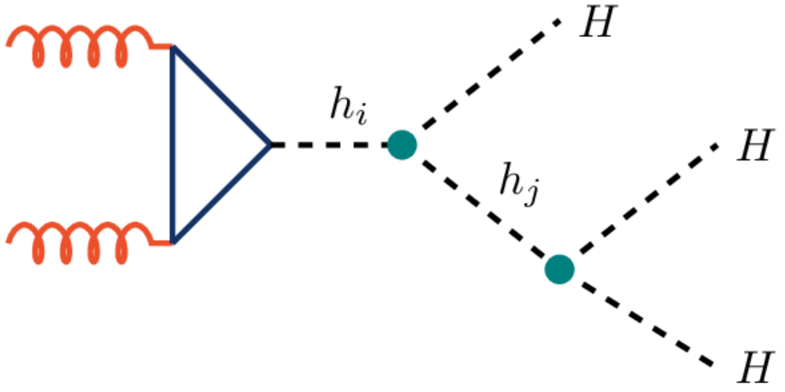

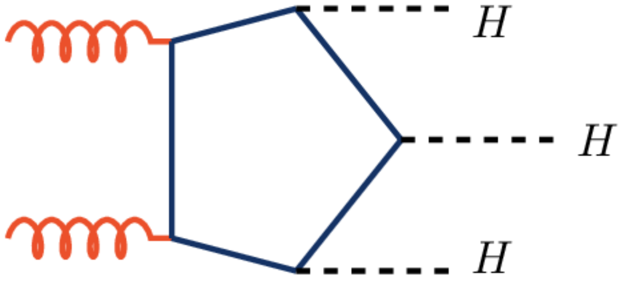

arXiv:2411.02040

HHH production - BSM

- Two Real Singlet Model (TRSM)
  - Extending the SM by adding two real scalar bosons ***X*** and ***S***.
  - LO productions reach cross-section values of ***up to ~ 50fb***.
  - Mass ranges: $m_X > m_S$, 325 < m_X <575 GeV, 200 < m_S <350 GeV (fulfill perturbative unitarity bounds).
  - Resonant + non-resonant, all LO ggF production modes (BSM + SM).
- Simple model for dark matter and CP violation (DM-CPV)
  - Dark matter is vector-like dark fermion.
  - Interacting with SM through scalars similar as the scalars in TRSM.
  - **Negligible differences** are found in the HHH event **kinematics between the TRSM and DM-CPV models**.

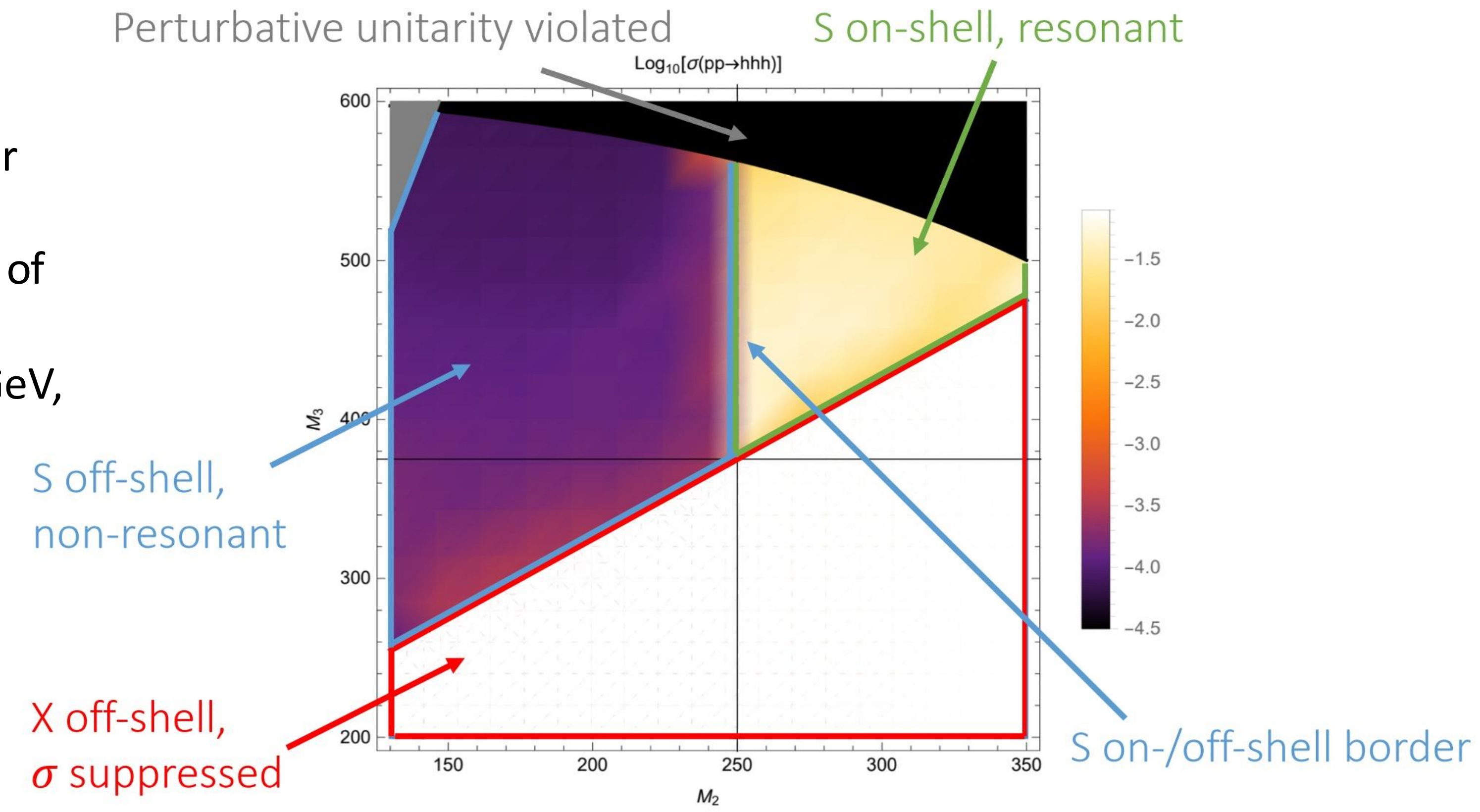

- Simplified TRSM model
  - TRSM breaks unitarity at high masses, and becomes dominated by the non-resonant diagrams. Simplify model to avoid TRSM problems.
  - Only consider **resonant ggF production** ($X \to SH \to HHH$).
  - $m_X > m_S$, 550 < m_X < 1500 GeV, 275 < m_S <1000 GeV.

Analysis overview

- Datasets: 126 fb^{-1}.
- **Three interpretations** based on the **kinematics** of the signal models.
  - **Non-resonant**: $m_S < 2m_H$ (250 GeV).
  - **Resonant**: $m_S > 2m_H$ (250 GeV).
  - **Heavy resonant**: generic heavy resonances (narrow & wide decay widths), m_S>275GeV, m_X > 550 GeV.
- Each search **follows the same general analysis strategy**.
- Dominant background: QCD multi-jet production. Estimate by **data-driven** method.
- A profile likelihood is performed on **Deep Neural Network (DNN) score** to obtain the final results.

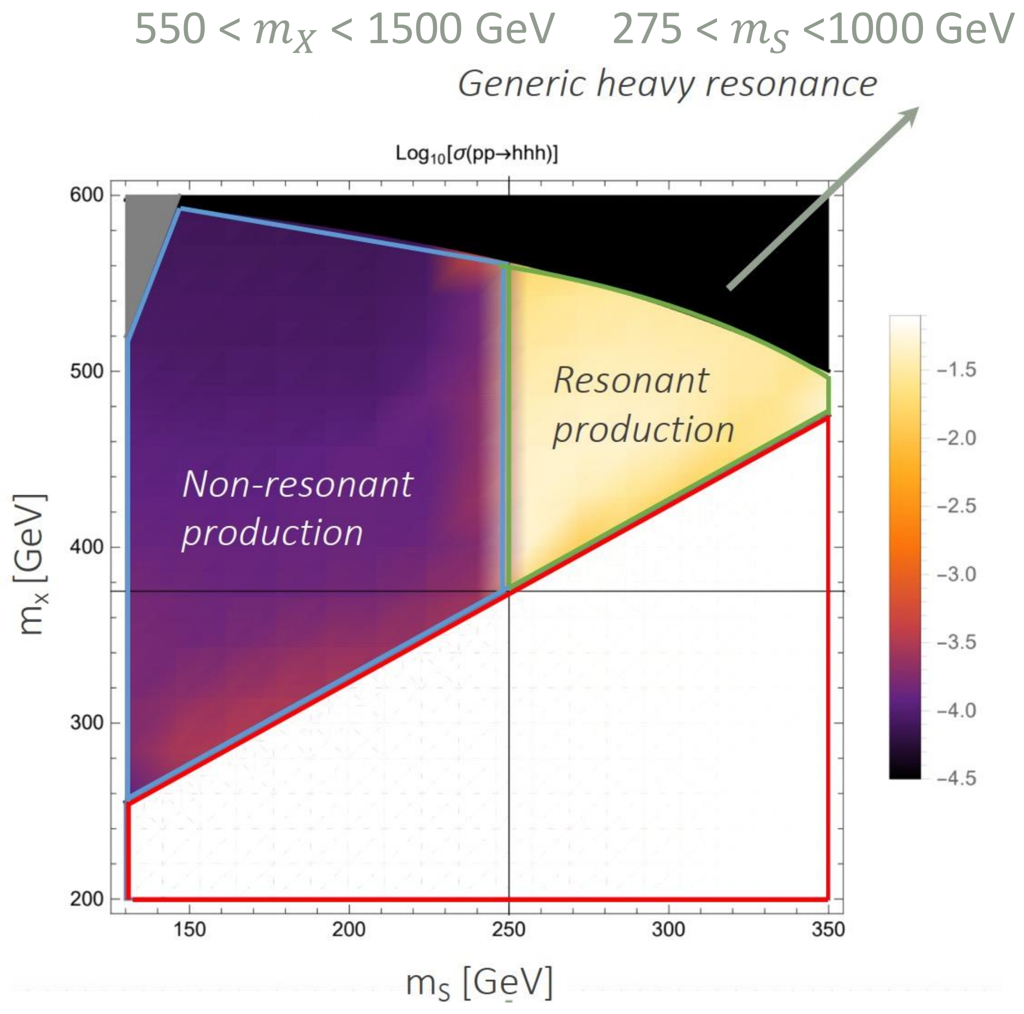

Event selection

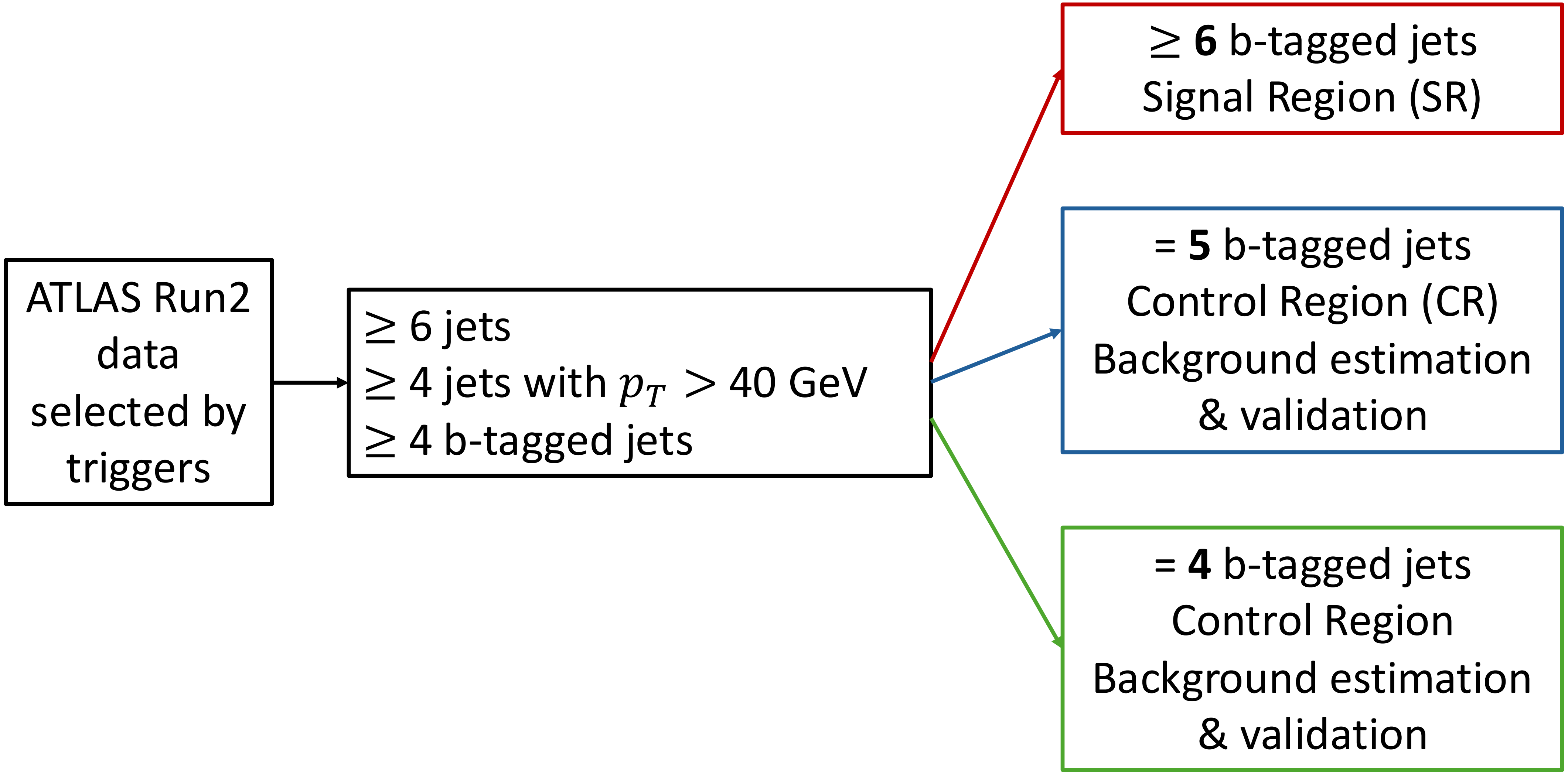

Jet pairing

- To help discriminate signal and background.
- Three Higgs boson candidates:

  6 jets are selected & paired. 15 ways to pair them.
- **Pairing algorithm:**

  minimizing $|m_{H1} - 120\ \text{GeV}| + |m_{H2} - 115\ \text{GeV}| + |m_{H3} - 110\ \text{GeV}|$

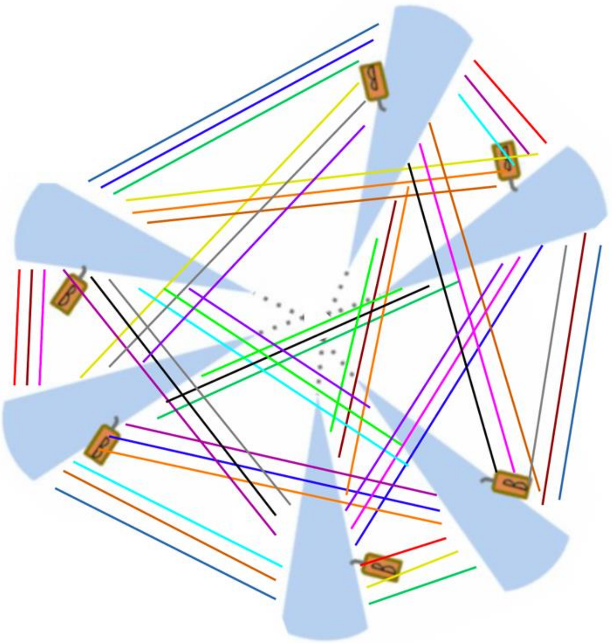

- Pairing efficiencies:

  SM-like ~ **60%**

  Resonant TRSM ~ **50%**

  Heavy resonant ~ **80%**

For 5b (4b) events:

For 6b events:

Deep Neural Network

- DNN output is used as the final discriminant.
- Training samples:
  - Background: 5b data
  - Signal: nonresDNN (6b SM HHH + 6b TRSM non-resonant), resDNN (all 6b resonant TRSM), heavyresDNN (all 6b heavy resonance)
- For each DNN, ten variables (good shape separation, minimal correlation with the b-jet multiplicity) are chosen as inputs.

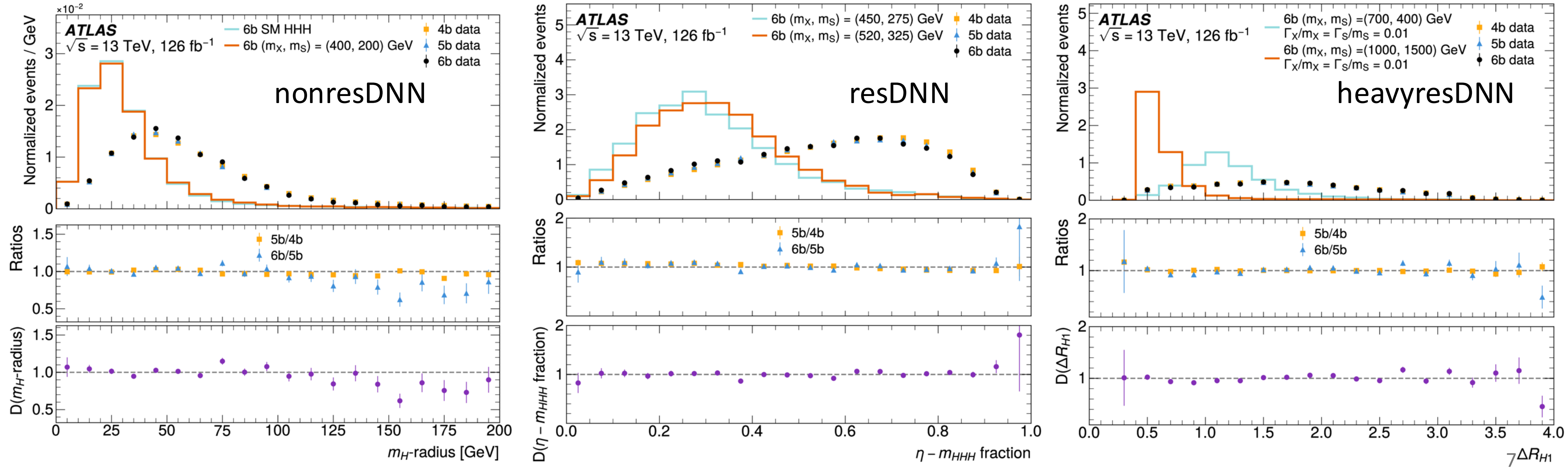

Background estimation

- Dominant background: QCD multi-jet production. Estimate by data-driven method.
- Assumption: kinematic properties of the background do not significantly change relative to b-jet multiplicity (validate by double ratio).
- Extrapolation: $4b \rightarrow 5b \rightarrow 6b(SR)$, extrapolate shape in b-tag multiplicity, normalized to 6b yields.
  - **Excluded region**: large shape difference between 4b, 5b and 6b, exclude from fit.
  - **Low-score region**: B-tag extrapolation, validate background estimate, derive shape systematics.
  - **High-score region**: 6b SR.

Double ratio: $\frac{R_{6b/5b}}{R_{5b/4b}} \sim 1$

Normalized to 6b yields

$$N_i^{6b,predicted} = N_i^{5b} \cdot \frac{N^{6b}}{N^{5b}} \cdot \frac{\left(N^{5b}/N^{4b}\right)_i}{N^{5b}/N^{4b}}$$

Extrapolate the shape of DNN score

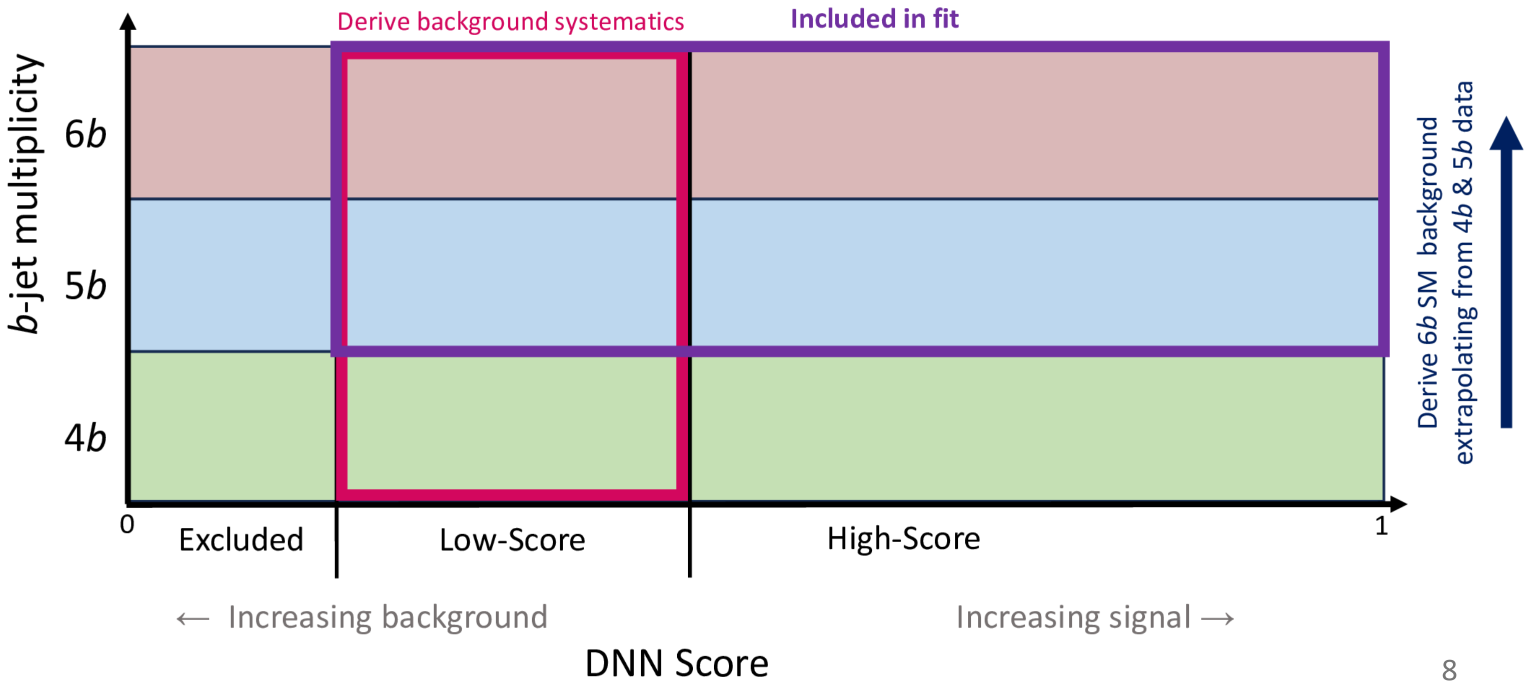

Uncertainties

Uncertainty source	Relative impact of systematic uncertainties [%]			
	SM-like	TRSM non-resonant	TRSM resonant	Heavy resonance
All uncertainties	24	20–46	33–42	24–53
Experimental	22	20–45	33–41	24–53
Detector response	7.4	6.6–14	16–24	4.1–15
Luminosity and pileup	<1	<1	<1	<1
Flavor tagging	3.2	2.8–5	6.9–8.8	1.5–5.6
Jet reconstruction	2.7	2.3–6.5	3.6–7.1	1.0–6.3
Trigger efficiency	2.0	1.8–3.5	6–10	1.4–4.2
Background modeling	16	14–36	18–30	20–45
Theoretical	1.5	<1	<1	<1
MC statistical	<1	<1	<1	<1

- Background shape uncertainty is the dominate one in experimental uncertainties. The expected limit are changed from 14% to 45%.
- Theoretical uncertainties: (α_s +PDF) & QCD scale.

Non-resonant & resonant interpretations

- In all cases, the observed data agree well with the background, and **no significant excess** is seen.
- In non-resonant interpretation: largest deviation is at $(m_X, m_S) = (550{,}200)$ GeV with 0.19σ.
- In resonant interpretation: signal strength $\mu = 0$.

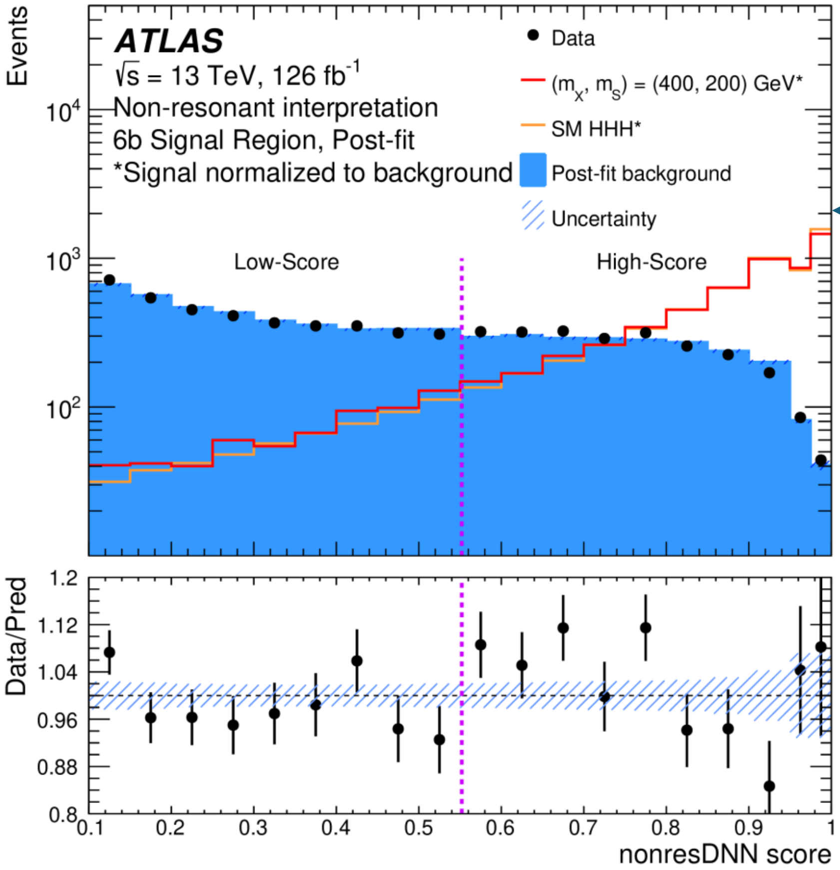

$(m_X, m_S) =$ (400,200) GeV

$(m_X, m_S) =$ (500,350) GeV

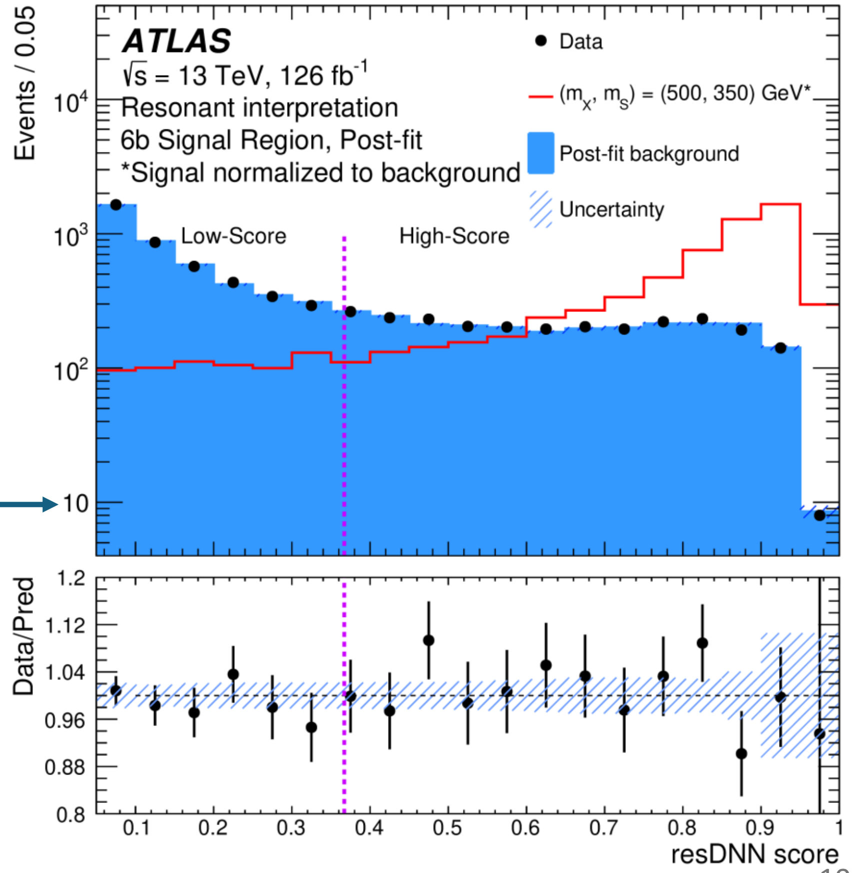

Non-resonant & resonant interpretations

- Cross-section upper limits in the (m_X, m_S) plane of non-resonant interpretation and resonant interpretation. (Observed: $48 \sim 310\ fb$.)

- SM HHH production:

$$\mu = \frac{\sigma_{HHH}}{\sigma_{HHH}^{SM}} \sim 750$$

Observed cross-section upper limit: $59 fb$

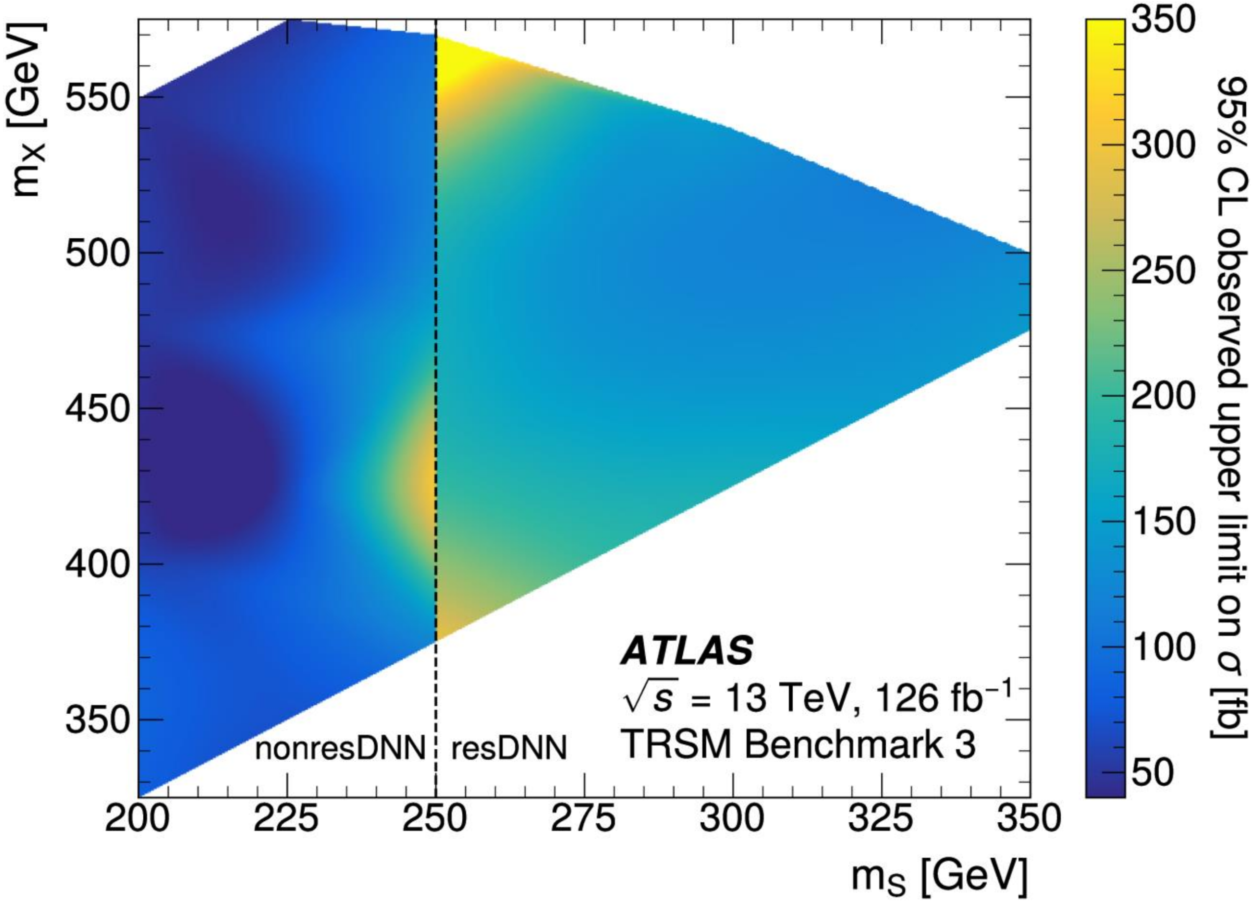

Heavy resonant interpretation

- In all cases, the observed data agree well with the background, and **no significant excess** is seen.
- In heavy resonant interpretation: largest deviation is at $(m_X, m_S) = (1500{,}275)$ GeV with 0.51σ.
- Observed limits for the narrow heavy resonance signals:

$5.7 \sim 38\ fb$

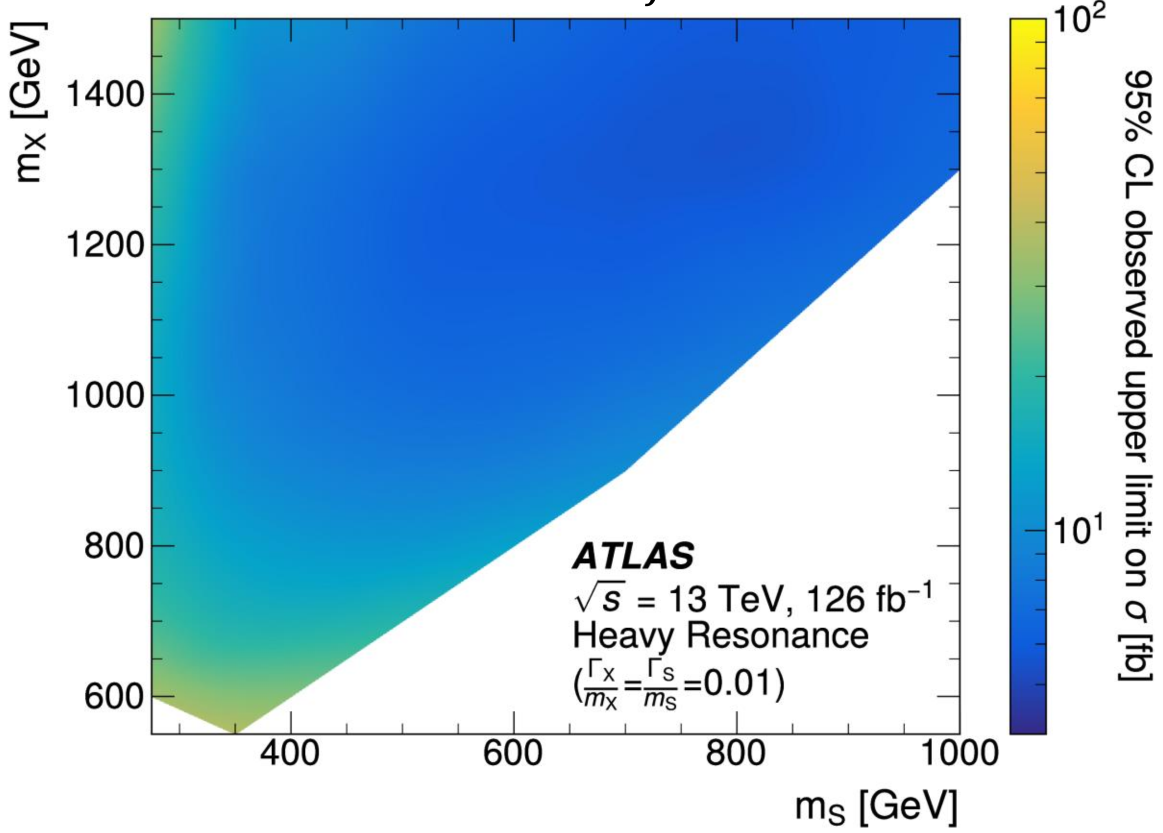

$(m_X, m_S) = (900{,}325)$ GeV

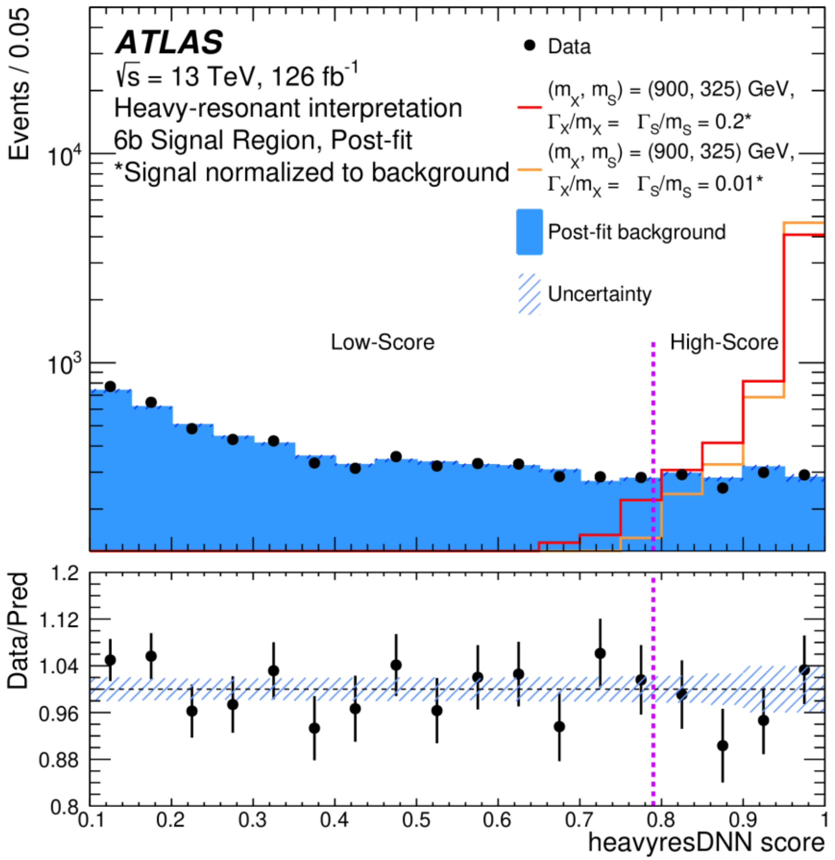

Heavy resonant interpretation

- In all cases, the observed data agree well with the background, and **no significant excess** is seen.
- In heavy resonant interpretation: largest deviation is at $(m_X, m_S) = (1500{,}275)$ GeV with 0.51σ.
- Observed limits for the wide heavy resonance signals:

$6.3\sim39\ fb$

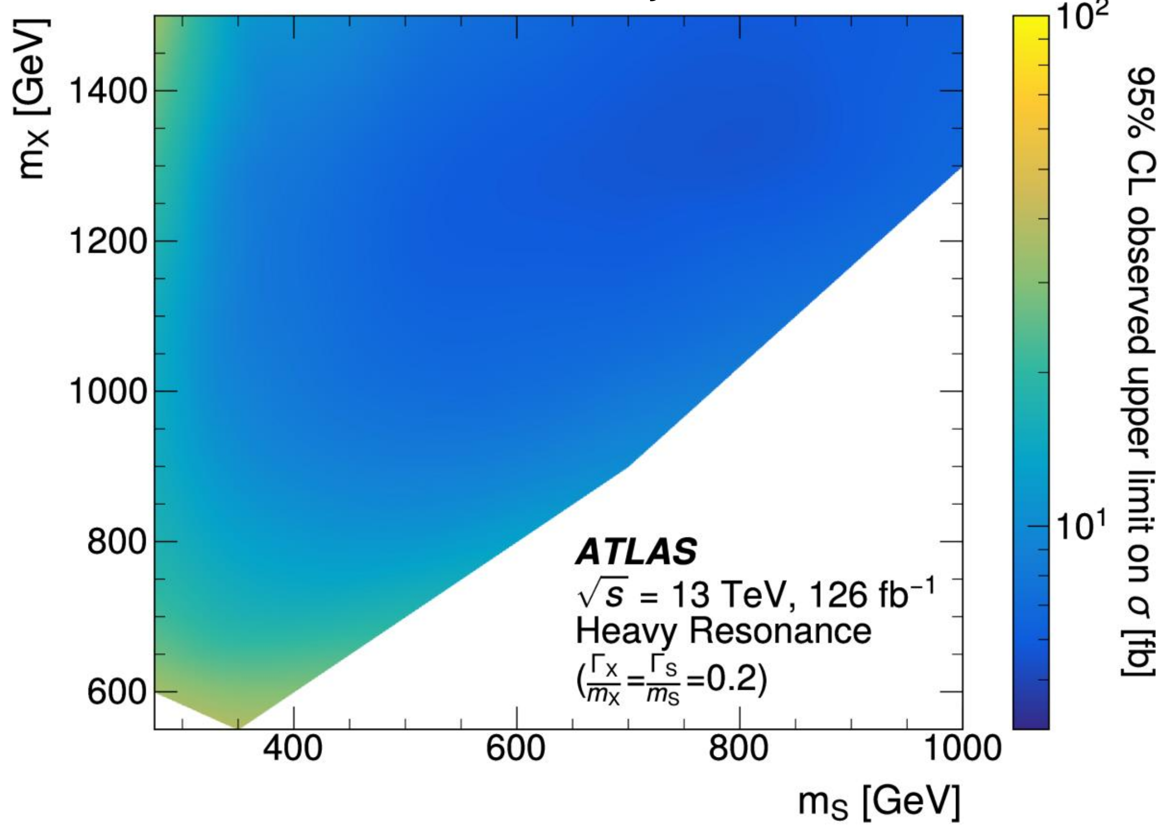

$(m_X, m_S) = (900{,}325)$ GeV

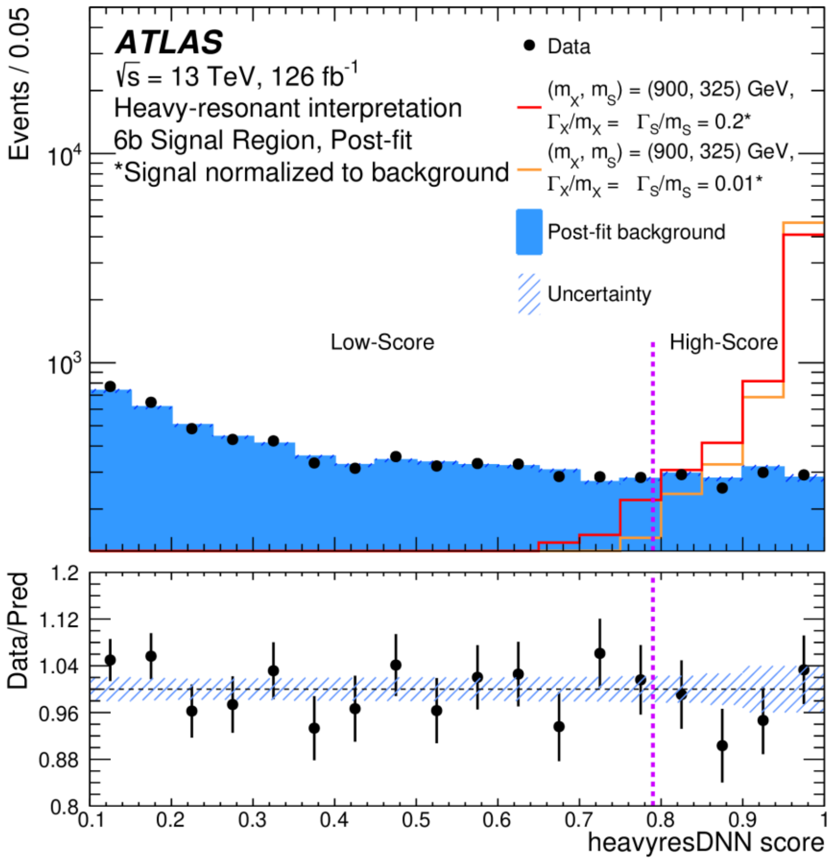

κ_3 and κ_4 scan

- **Constraints on quartic coupling** set for the first time.
- Degeneracy of $\sigma_{HHH}(\kappa_3, \kappa_4)$.
- At the 95% CL none of the phase space inside the unitarity bounds is excluded.

In the SM: $\kappa_3 = \kappa_4 = 1$

Assuming $\kappa_4 = 1$, κ_3: $-11{\sim}17$ at 95% CL.

Assuming $\kappa_3 = 1$, κ_4: $-230{\sim}240$ at 95% CL.

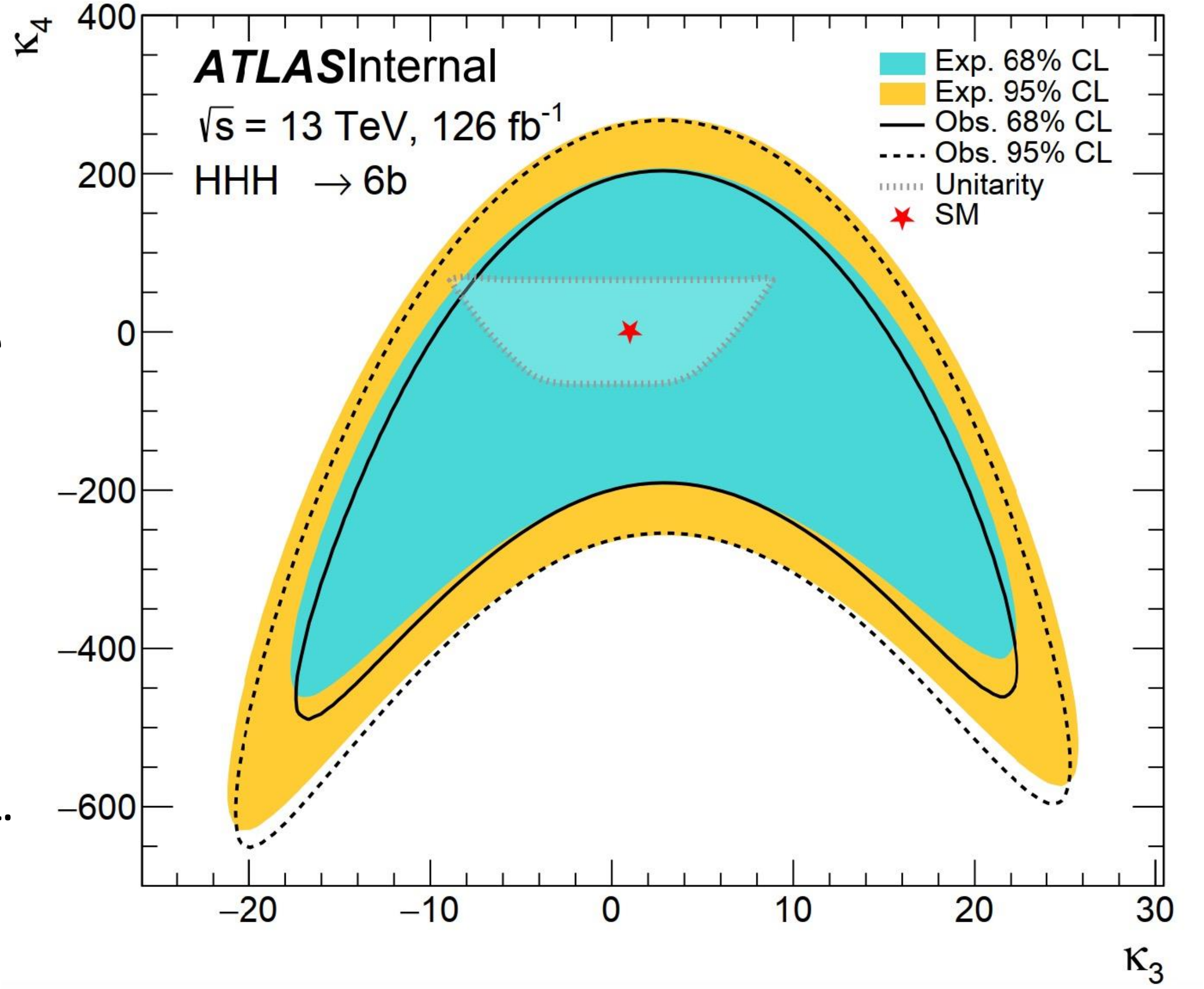

Summary

- Search for tri-Higgs production in 6b final state with $126 fb^{-1}$ ATLAS run2 data. It's the **first search of such topology at the LHC!**
- Three different DNNs are used in **non-resonant** (including a search for SM like signals), **resonant** and **heavy resonant interpretations**. Data-driven method is used to estimate background.
- **No significant excess observed** in the search for SM like and various BSM signals. Constrains of κ_3 and κ_4 (**for the first time**) are presented.

arXiv:2411.02040

- Relevant talk in Higgs Potential 2024:

Higgs Potential From Standard Model to EFT and UV Models – Hao-Lin Li

上海交通大學
SHANGHAI JIAO TONG UNIVERSITY

ATLAS
EXPERIMENT

李政道研究所
Tsung-Dao Lee Institute

谢谢！

TRSM structure

The "cascade" diagram dominate in TRSM parameter space

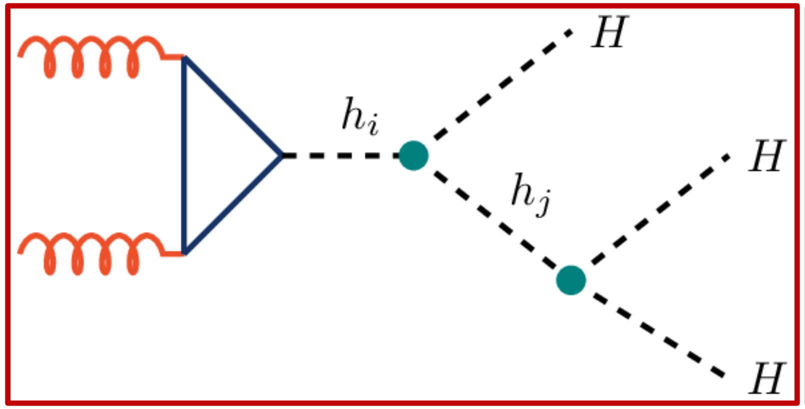

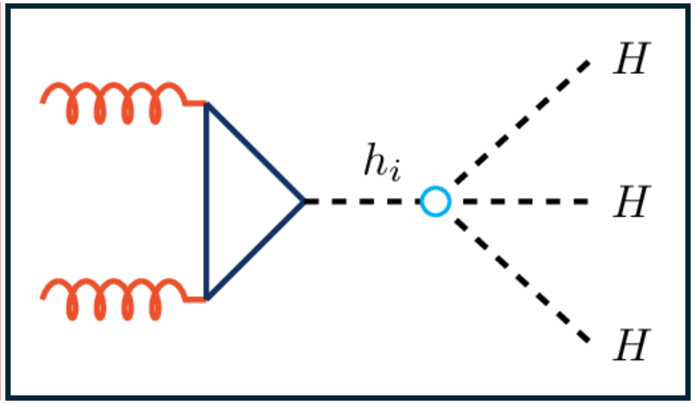

This diagram is generally sub-dominate, but not quite negligible.

The semi-/non-resonant diagrams are small

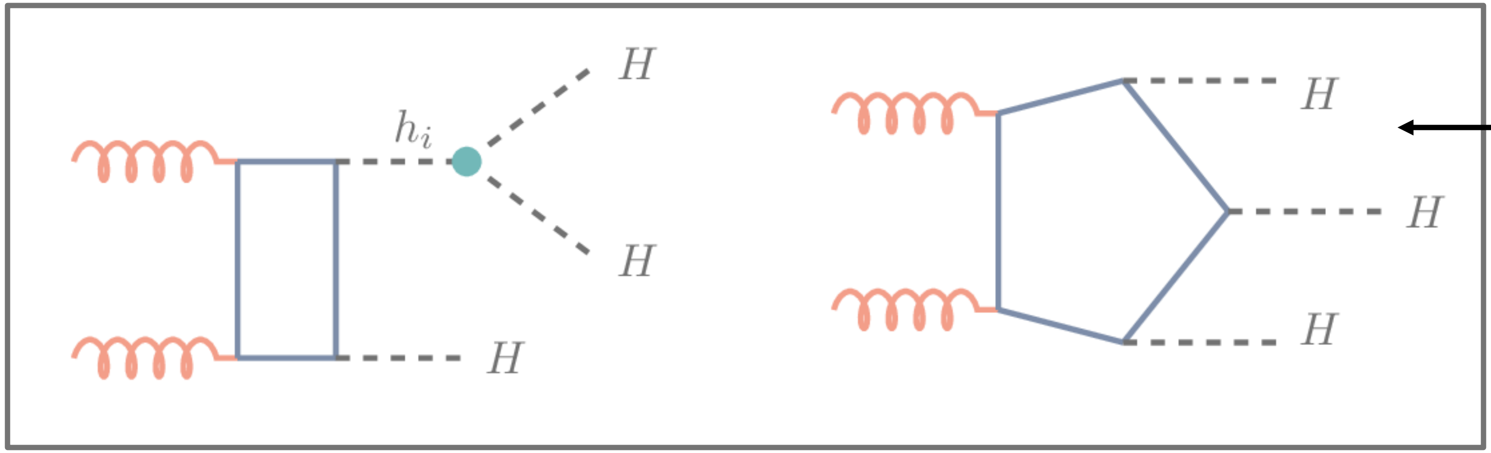

SM diagram

Object definition

Probe 6b final state

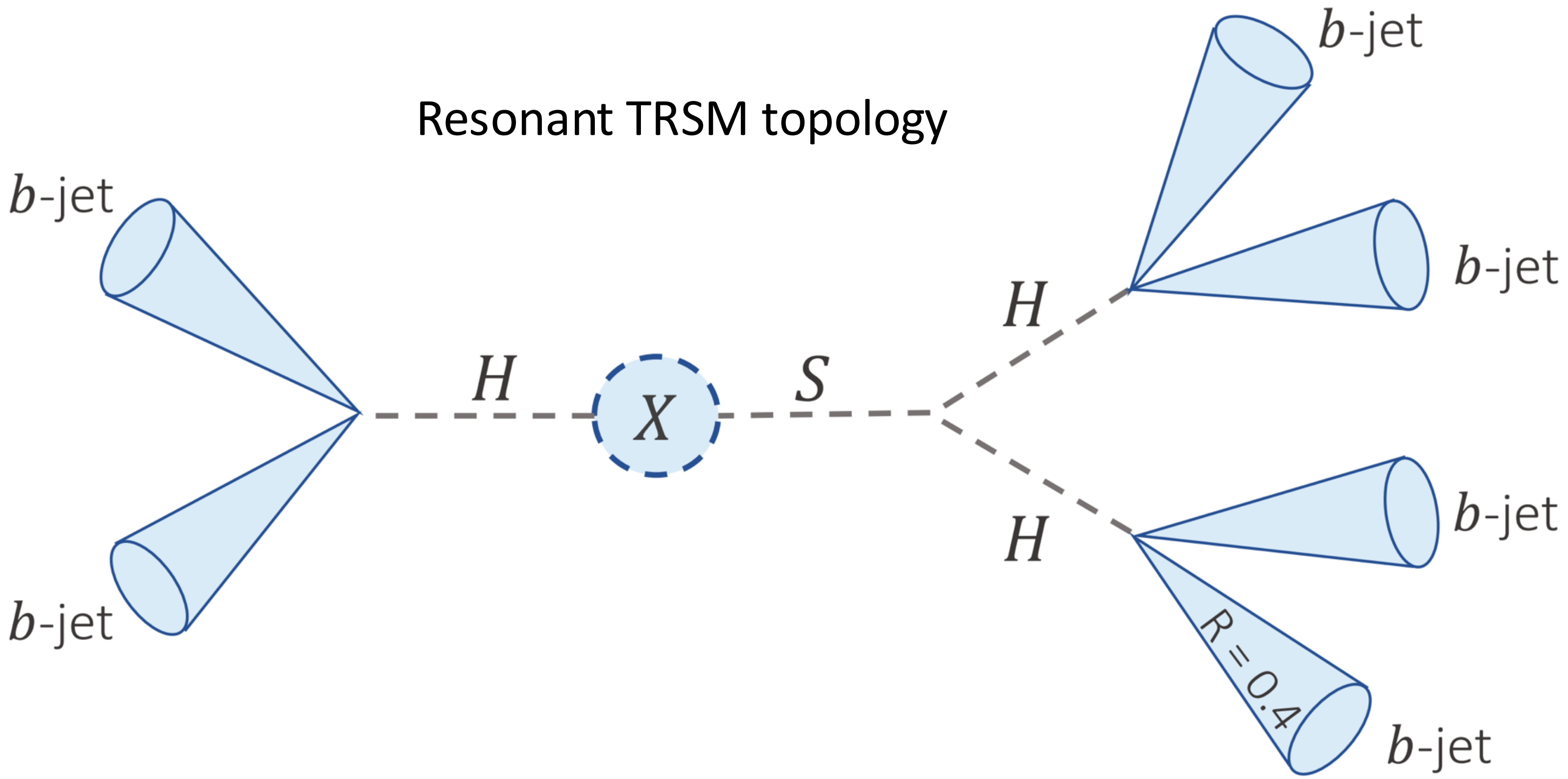

PFlow jets, $p_T > 20$ GeV, $|\eta| < 2.5$
B-tagged by DL1d 77% working point
μ-in-jet correction for semi-leptonic b-hadron decay

Jet pairing efficiency

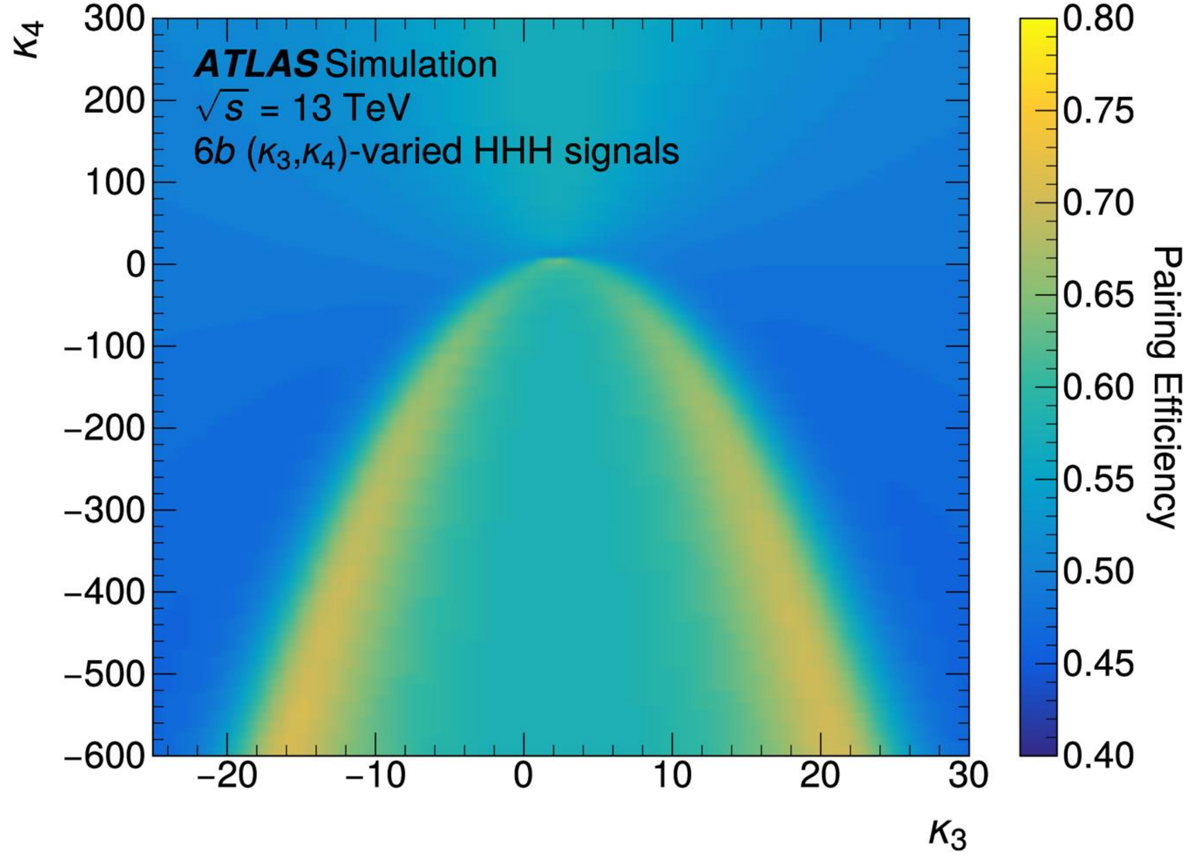

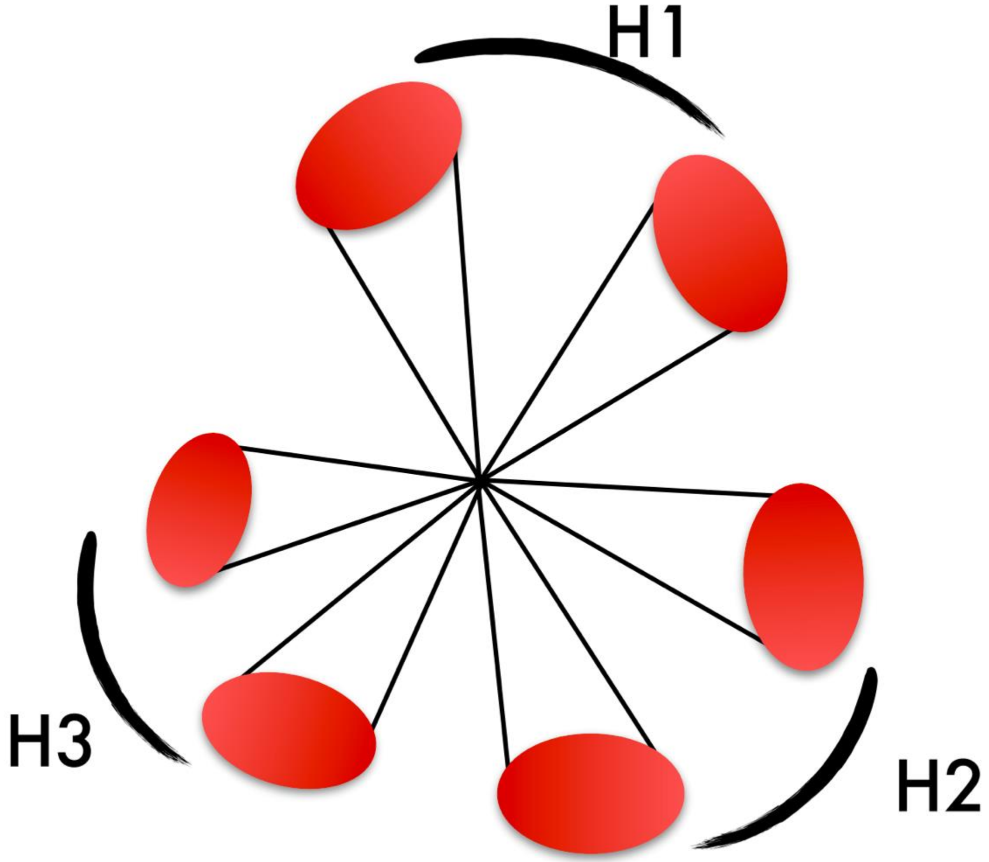

Jet pairing efficiency

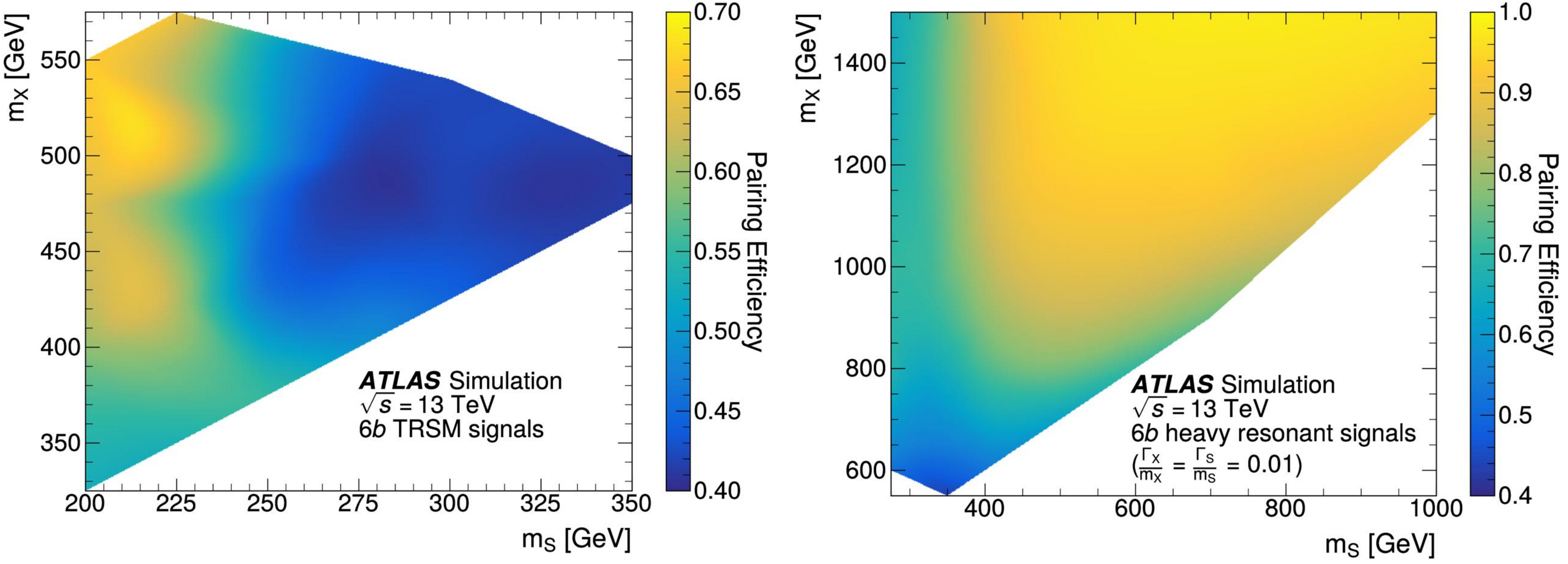

DNN

Variable	Definition	nonres	res	heavyres
m_H-radius	Euclidean distance between the event and the pairing center (120, 115, 110) GeV in the (m_{H1}, m_{H2}, m_{H3}) volume.	✓		✓
m_{H1}	Reconstructed mass of the highest p_T Higgs boson candidate.	✓		✓
RMS(m_{jj})	Root-mean-squared (RMS) of the invariant mass of all possible jet pairs that can form a Higgs boson candidate.	✓		✓
RMS(ΔR_{jj})	RMS of the angular separation between all possible jet pairs that can form a Higgs boson candidate.	✓	✓	✓
RMS(η)	RMS of the pseudo-rapidity of the Higgs boson candidates.	✓		✓
Skewness ΔA_{jj}	Skewness of $\cosh(\Delta\eta_{ik}) - \cos(\Delta\phi_{ik})$, where i, k are all possible jet pairs that can form a Higgs boson candidate.		✓	
H_T^{6j}	Scalar sum of the p_T of the 6 jets selected to reconstruct the 3 Higgs boson candidates.		✓	
$\cos\theta$	In the (m_{H1}, m_{H2}, m_{H3}) coordinate system, θ is the angle between the vector from the origin to the event's reconstructed mass of the Higgs boson candidates, and the vector from the origin to (120, 115, 110) GeV.		✓	
Aplanarity$_{6j}$	The fraction of p_T from the 6 jets selected to reconstruct the 3 Higgs boson candidates lying outside the plane formed by the 2 highest p_T jets.	✓	✓	✓
Sphericity$_{6j}$	Isotropy of the momenta of the 6 jets selected to reconstruct the 3 Higgs boson candidates.		✓	
Transverse Sphericity$_{6j}$	Isotropy of the p_T of the 6 jets used for Higgs reconstruction, within the $x-y$ plane.	✓		
Sphericity	Isotropy of the momenta of all jets in the event.			✓
$\eta - m_{HHH}$ fraction	$\frac{\sum_{i,k} 2p_T^i * p_T^k * (\cosh(\Delta\eta(ik))-1)}{m_{HHH}^2}$ where i, k are all possible jet pairs that can form a Higgs boson candidate, and m_{HHH} is the reconstructed tri-Higgs invariant mass.		✓	
ΔR_{H1}	Angular separation between the jets paired to form the highest p_T Higgs boson candidate.	✓	✓	✓
ΔR_{H2}	Angular separation between the jets paired to form the second-highest p_T Higgs boson candidate.	✓	✓	✓
ΔR_{H3}	Angular separation between the jets paired to form the lowest p_T Higgs boson candidate.	✓	✓	✓

Background estimation

- The non-closure in the extrapolation method in low-score region is used to estimate the systematic uncertainty.

$$D(\nu)=\frac{\left(N^{6b}/N^{5b}\right)_{(\nu)}}{N^{6b}/N^{5b}}\div\frac{\left(N^{5b}/N^{4b}\right)_{(\nu)}}{N^{5b}/N^{4b}}$$

ν:DNN input variables

- The shape variations are always smaller than the statistical uncertainty.

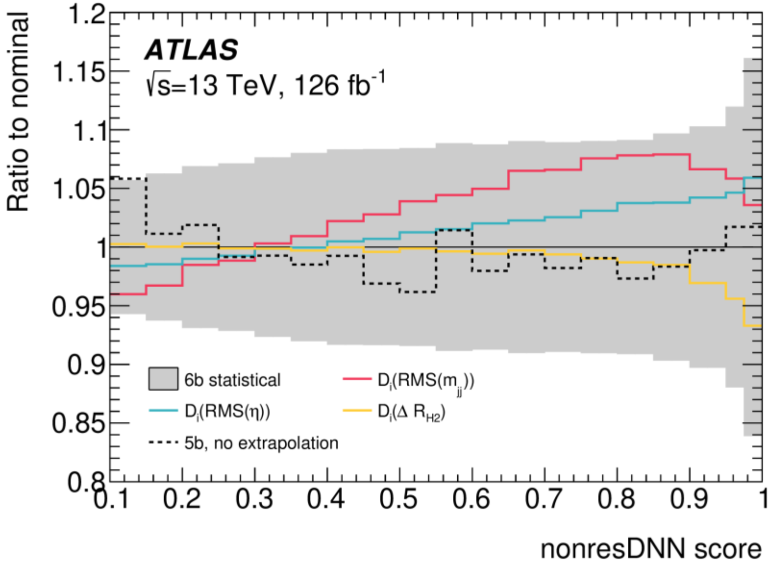

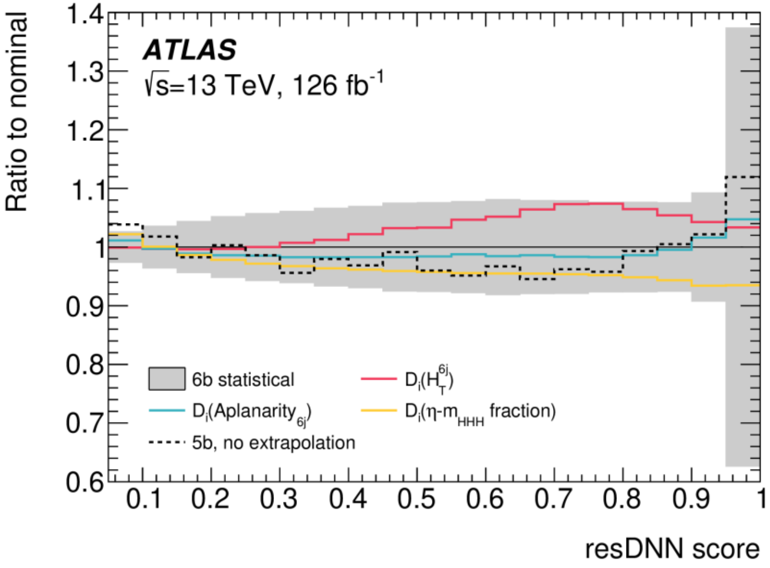

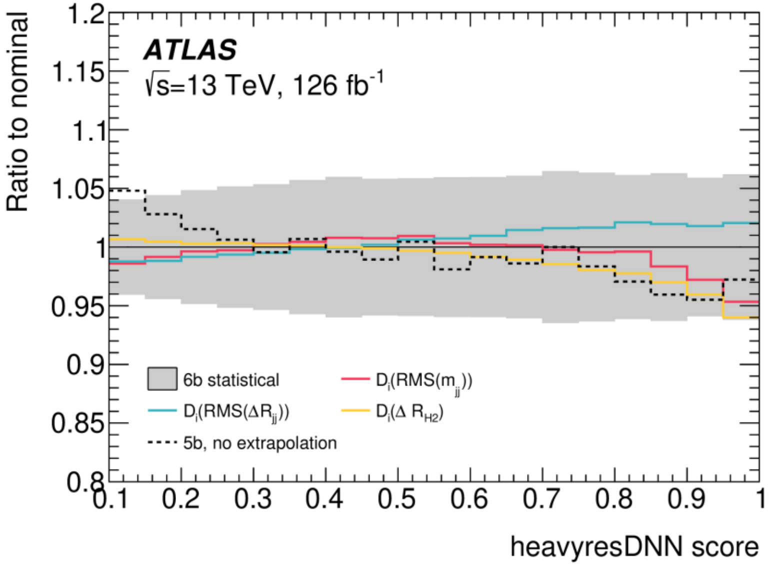

Non-resonant & resonant interpretation

- Cross-section upper limits in the (m_X, m_S) plane of non-resonant interpretation and resonant interpretation.

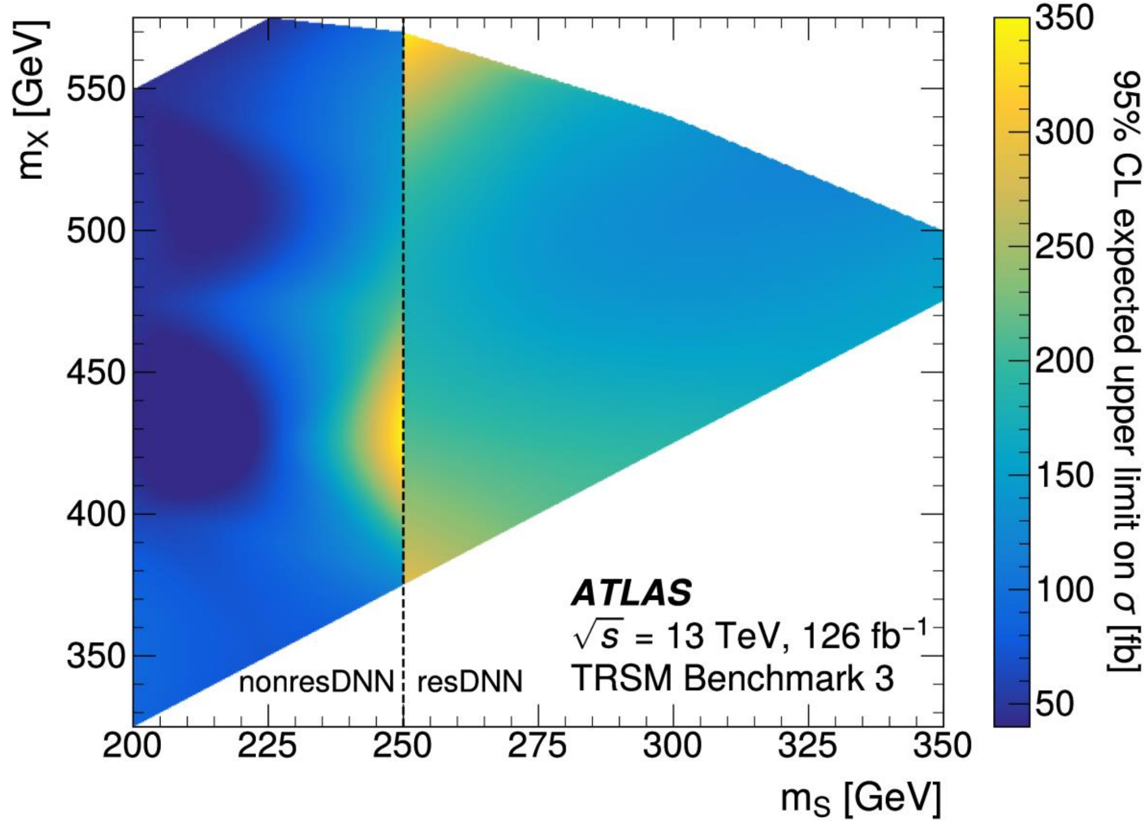

Expected: $46 \sim 350\ fb$

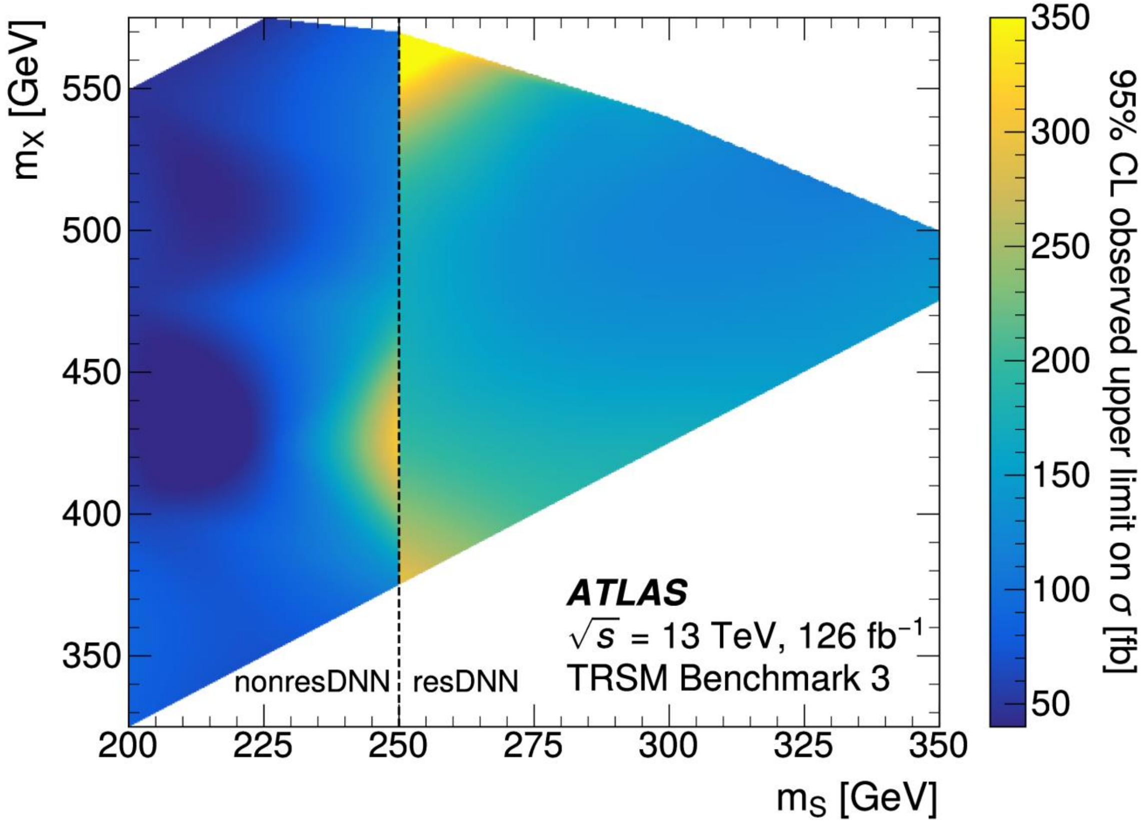

Observed: $48 \sim 310\ fb$

Self-coupling interpretation

- Theoretical dependence on κ_3 and κ_4.

Papaefstathiou, Tetlamatzi-Xolocotzi, Zaro (1909.09166)

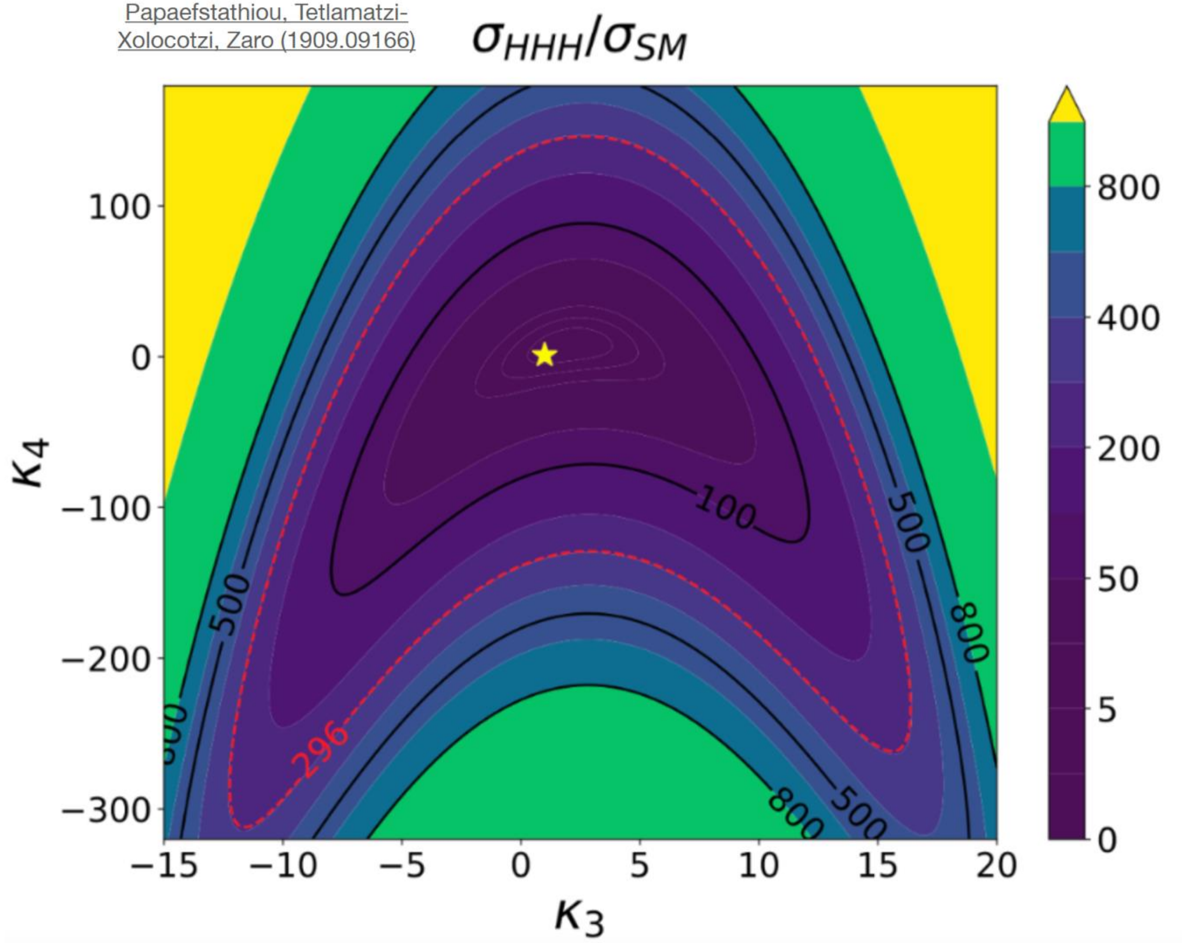

$$\frac{\sigma(c_3,d_4)_{hhh}}{\sigma(\mathrm{SM})_{hhh}} - 1 = 0.0309 \times c_3^4 - 0.2079 \times c_3^3 + 0.0407 \times c_3^2 d_4 + 0.7384 \times c_3^2 + 0.0156 \times d_4^2 - 0.1450 \times c_3 d_4 - 0.1078 \times d_4 - 0.6887 \times c_3 \,.$$

$$c_3 = \kappa_3 - 1$$

$$d_4 = \kappa_4 - 1$$

In SM: $\kappa_3 = \kappa_4 = 1$

$\sigma_{\mathrm{HHH}}^{min}(\kappa_3, \kappa_4)$: $\kappa_3 \sim 2$, $\kappa_4 \sim 8$

$\sigma_{\mathrm{HHH}}^{min}(\kappa_3, \kappa_4 = 1)$: $\kappa_3 \sim 1.6$

$\sigma_{\mathrm{HHH}}^{min}(\kappa_3 = 1, \kappa_4)$: $\kappa_4 \sim 4.5$